SEMARAK ILMU PUBLISHING

CFD Letters

Journal homepage:
https://semarakilmu.com.my/journals/index.php/CFD_Letters/index
ISSN: 2180-1363

Transient Analysis on the Crosswind Effect to the Aerodynamics of High-speed Train Travelled on the Bridge Between Two Tunnels at Jakarta - Bandung Track

Harinaldi[1,*], Farhan T Pratama[1]

[1] Department of Mechanical Engineering, Faculty of Engineering, University of Indonesia, Depok 15424, Indonesia

ARTICLE INFO

Article history:
Received 5 November 2023
Received in revised form 7 December 2023
Accepted 10 January 2024
Available online 31 May 2024

Keywords:
high speed train; crosswind; aerodynamics coefficient; CFD simulation; tunnel – bridge

ABSTRACT

The rapid evolution of global transportation technology is exemplified by Indonesia's innovative high-speed train initiative, linking Jakarta and Bandung in an impressive 45 minutes. Operating at 350 km/h, the HST CR400AF underscores the importance of aerodynamics in high-speed rail systems. This study delves into the significant impact of crosswind on key aerodynamic factors (drag, lift, rolling moment) within the tunnel-bridge-tunnel configuration. Leveraging Computational Fluid Dynamics (CFD) through ANSYS FLUENT, the analysis explores crosswind variations at 0 m/s, 10 m/s, and 25 m/s. Results reveal a proportional increase in aerodynamic load with higher crosswind intensities: 1.67 times for drag, 58.8 times for lift, and 29.8 times for rolling moment. Notable observations include pronounced aerodynamic load fluctuations during the "OUT" process, with the head section bearing the greatest load, followed by the tail and middle sections. These findings contribute valuable insights to the global discourse on enhancing safety and efficiency in high-speed rail systems.

1. Introduction

Indonesia with a population of 272.23 million in the year 2021 has a population distribution centered on the island of Java. There are around 152 million people with an area of 7% of the total territory of Indonesia. The capital city of Jakarta and the city of Bandung are the most densely populated cities with transportation infrastructure problems. According to reports by Ginés [1] currently high-speed trains have been considered one of the most significant technological breakthroughs in the development of passenger transport in the 20th century. In that regards, Indonesia decided to adopt the high-speed train in the Jakarta - Bandung coridor and a high-speed train corporation, namely PT Kereta Cepat Indonesia China (PT KCIC) was established to solve Jakarta – Bandung traffic problem. The railways track has a total length of 142.3 km stretching from Jakarta to Bandung with four stopping stations and 80 km of track consists of elevated track while the rest consists of tunnels and other varied terrain.

* *Corresponding author.*
E-mail address: harinaldi.d@ui.ac.id (Harinaldi)

https://doi.org/10.37934/cfdl.16.10.6480

When the train enter the tunnel, a different aerodynamic phenomenon to the conditions of open-air will occur. It will give a significant rise to the pressure conditions in the tunnel, also called the piston effect as mentioned by Baker [2]. Furthermore, there is another more extreme case that allows more complex aerodynamic phenomena to occur. It is when the train passing through two tunnels connected by a bridge [3]. In Jakarta-Bandung high-speed train track, this configuration is located in the Walini area precisely on tunnel 7 – bridge – tunnel 8 Walini as shown in Figure 1.

Fig. 1. Tunnel – bridge – tunnel scheme in Walini, West Java province

The works of Li, *et al.,* [4] explained that the bridge is a facility that is vulnerable to strong winds because it is the main route of airflow. When the wind combines with the train speed it will produce a relative wind which creates a crosswind effect on the train [5]. The aerodynamic forces and moments due to crosswind have a significant impact on the stability of the fast train and increase the risk of overturning. Baker [6] reported that the effect is an instant increase in the aerodynamic coefficient in the crosswind. Due to the reasons above, many studies have been carried out such as wind tunnel tests and numerical simulations. Cheng, *et al.,* [7] analyzed the safety and stability of high-speed trains in a crosswind. Deng, *et al.,* [3] conducted a study on transient aerodynamic phenomena that occurred in the tunnel – bridge-tunnel in China with a numerical simulation method. The method and boundaries in the simulation have been verified with the results of experiments conducted by Wan and Wu [8] and also by Han and Tian [9]. The difference between the simulation and experimental results were less than 5%.

In the current work, we investigate the aerodynamics phenomenon in the Jakarta-Bandung high-speed train track which is located at tunnel 7-bridge-tunnel 8 segment in the Walini area which is vulnerable to a crosswind. The analysis is carried out using aerodynamics coefficients of the rolling moment, and lift, which have a significant role in the occurrence of train overturning. For clarity drag coefficient analysis during entering tunnel is also included. The research use a replica of the CR400AF train model running at designed operational speed of 350 km/h shown in Figure 2(a) and (b).

(a) (b)

Fig. 2. Comparison between the (a) real CR400AF train and (b) 1:20 simplified model for numerical simulation

Numerical simulation is carried out to obtain the aerodynamics coefficients and pressure distribution of the fast train due to crosswind on the bridge between the two tunnels. The simulation method follows the schemes mentioned by Deng, *et al.,* [3, 5], Yang, *et al.,* [10], and Chen, *et al.,* [11] with some adjustments to match environmental adaptation in the Wallini area, West Java, Indonesia.

This research aims to analyze the phenomena that occur in the bridge area between two tunnels on the changes in aerodynamic coefficients and the pressure distribution that occurs when a high-speed train passes through a bridge between two tunnels. The investigation explores the behaviors of some aerodynamics phenomenon occur on the high-speed train, including rolling moment, lift, and drag when the train entering "IN" and exiting "OUT" from the tunnel with pressure distribution to support analysis when entering “IN” and leaving “OUT” the bridge. The analysis of the results is expected to be usefull in deriving further informations to safety measures of the Jakarta-Bandung high-speed train operation.

2. Methodology

2.1 Geometry

Prior to carrying out the simulation, the authors ensured that the 1:20 scale in the simulation could be used. According Niu, *et al.,* [12] the scaling performed on the high-speed train simulation does not have a significant difference and has an error below 2% as long as the Reynolds number (Re) is very large so that it has entered the "self-modelling region". In this regards, the current investigation continued to use a speed of 350 km/h in the simulation.

The high-speed train model was created using 2D photo analysis method. The train has two locomotives and one carriage with a total length (L) of 79.4 m consisting of a head and tail 27.2 m and a middle 25 m. The train design is only the body, not equipped with details such as windows, pantographs, wheels, etc. The train was located on the windward of the double-track because when it comes to crosswind environment there are more disadvantageous when running on the windward rather than on the leeward side [13]. The tunnel diameter of the Jakarta-Bandung high-speed rail project was found to be 11.8 meters wide. Niu, *et al.,* [14] suggested that the length of the tunnel for such kind of simulation only need 2.63 L to represent the state in the whole tunnel, where L is the length of the train. The bridge has a total width of 12.4 m with a length of 580 m. The design made several simplifications on the corners and side walls of the bridge.

As shown in Figure 3, overall, there are four parts to be assembled, namely: (1) Open air (OA) flat rail representation with the length of region OA was 2.63 L; (2) tunnel 1 (T1) represents tunnel 7; (3) Boundary Region (BR) along with boundary conditions on the bridge. In this section, there is also a crosswind with a direction perpendicular to the bridge; and (4) tunnel 2 (T2) represents tunnel 8 Walini. The boundary condition on OA and T2 (at the end) was set to be pressure-outlet condition. The cylinder BR surface was set to pressure-far-field boundary condition to help generate crosswind by using Mach number. Crosswind and velocity of the train were assumed to have a uniform flow.

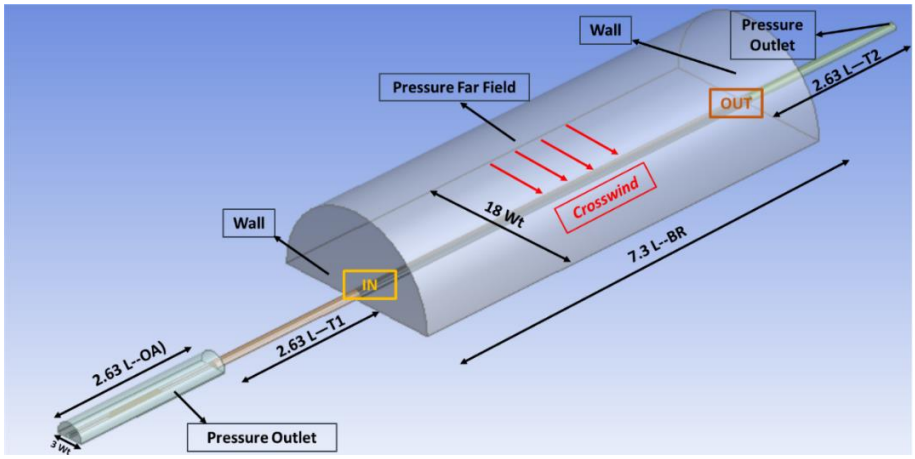

Fig. 3. Geometry of computational domain and boundary conditions

2.2 Meshing Strategy

Using the design modeler in ANSYS FLUENT, the assembly was grouped up into two zones, namely, the dynamic zone and the static zone as shown in Figure 4. To realize the flow field data between two regions, interface pairs were used in this simulation. Dynamic zones consist of the CR400AF model and the air nearby the train. The environment like the tunnel, bridge, and boundary were grouped into a static zone. Adopting the works by Deng, *et al.,* [3] and Yang, *et al.,* [15], the dynamic layering mesh method was performed to realize relative motion between the ground and the train. The speed of the train (V_t) was generalized using mesh motion in dynamic zones.

Two different methods of meshing were performed in this simulation. The multizone mesh method with hexa-core mesh and tetrahedron as a free mesh type was used in the static zone. The dynamic zone was meshed using the patch conforming method due to the complexity of train geometry. To get the most efficient number of cells, an adaptive sizing mesh was applied. Geometry that has high complexity like train and bridge had to use defeaturing size of 1.6×10^{-4} to get the finest shape of the mesh. Boundary layers were used to minimalize the effect of the flow field between the two regions with a first layer thickness of 3×10^{-4} and the growth rate set to 1.2, 8 and 15 boundary layers were set into the bridge and the train [16]. The element size of static zones were 6×10^{-2} and 2×10^{-2} for the dynamic zone were used in this simulation. From all the methods above, the skewness metrics score was average in 0.22.

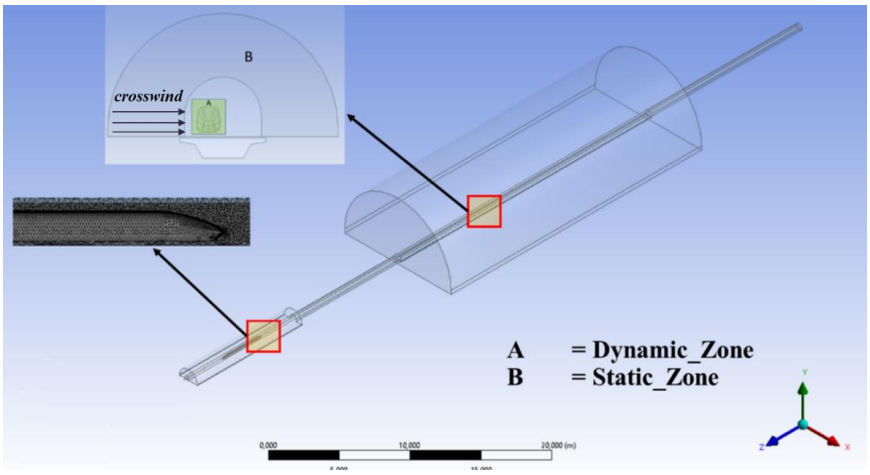

Fig. 4. Schematic of simulation model

2.3 Computational Setup and Governing Equation

To determine the setup to be carried out, it is necessary to know some basic conditions icluding the Reynolds number and speed contained in the simulation. In this case the Reynolds number hits 10^6 and the train speed is 0.28 Mach Number. Other considerations such as the compression that occurs in the air in the tunnel must also be considered in determining the behaviour of the air in the simulation [10]. From some of the considerations above, ideal compressed air was used because there was compression as the train speed was close to 0.3 mach.

In this simulation, the Reynolds Averaged Navier Stokes (RANS) method was used. This was done because of the efficiency provided by the RANS method itself [14]. The RANS method makes the efficiency of the simulation increased, this is very much needed considering the limitations of the computations it has. The turbulence model in the RANS method is also widely used to simulate structural flow and pressure distribution in each case which is very representative in this study. The development of the RANS formula was adapted from the continuity and momentum equations which can be described as follows:

$$\frac{\partial \rho}{\partial t} + \frac{\partial}{\partial x_i}(\rho u_i) = 0 \tag{1}$$

$$\frac{\partial}{\partial t}(\rho u_i) + \frac{\partial}{\partial x_j}\left(\rho u_i u_j\right) = -\frac{\partial \rho}{\partial x_i} + \rho g \delta_{i3} + \frac{\partial}{\partial x_j}\left[\mu\left(\frac{\partial u_i}{\partial x_j} + \frac{\partial u_j}{\partial x_i}\right) - \frac{2}{3}\delta_{ij}\frac{\partial u_i}{\partial x_i}\right] + \frac{\partial}{x_j}\left(-\rho u_i' u_j'\right) \tag{2}$$

Many turbulences models from RANS have been calculated in high-speed train simulations. Study of Lu, *et al.,* 2020 [17] used the RNG k-ε turbulent method as a calculation in the simulation. Abdel Gawad, *et al.,* [18] applied the realizable k-ε turbulence model in their simulations on aerodynamic noise of high-speed train. Research by Wang, *et al.,* [19] uses SST k-ω in calculations that compare the RANS, SAS, and DES methods. The consideration of using the turbulence method in this simulation is obtained from two approaches, namely: (1) Observing the phenomena that occur in the process of entering and leaving the tunnel, and (2) Observing the phenomena that occur when on the bridge. From the two considerations above in this study will use the SST k-ω turbulence method.

Computational simulation used the ANSYS FLUENT 21.1 to elucidate the phenomenon that occur due to crosswind on high-speed trains. The simulation was carried out using the transient method so that the phenomenon could be more clearly seen when a train running across the bridge. The simulations was carried out with a train speed of 350 km/h at variations of crosswind speeds of 0 m/s, 10 m/s and 25 m/s. The simulation used a pressure-based solver, this was because the air velocity does not exceed 0.3 Mach number so that pressure was the input. The solver method used a pressure implicit scheme with an implicit second order level. The pre-setup preparation provided input on the CR400AF's carriage area and the speed at which it was applied. The total length of the simulation geometry was 53.5 m, so it took about 0.55 seconds for the train to travel the distance from the open area (OA) to the tunnel (T2). The time step size used was 1×10^{-3} s. Many of the high-speed train studies use similar or even larger time step sizes with values ranging from 1×10^{-3} s to 7×10^{-3} s [15]. With the selection of the time step size, the current investigation required 550 number of time steps. The number of iterations per time step was 20 and the residual set for each time step was 10^{-3}.

2.4 Aerodynamics Coefficient Calculations

Aerodynamic resistance can be experienced by an object moving through air fluid. In all cases, the effect of the distribution of pressure and shear stress on the entire surface of the object is the resultant aerodynamic forces and moments on the object. High-speed trains traveling in a crosswind will experience greater aerodynamic loads due to normal stresses and tangential stresses to the train surface as shown by Ishak, *et al.,* [20]. Forces and moments such as drag force, lift force, side force, rolling moment, pitching moment, and yawing moment will affect the speed of a high-speed train. The performance of these forces and moments has their respective roles and directions as shown in Figure 5. Aerodynamic coefficients such as listed in Tabel. 1 were also used to analyze the phenomena that occur on the bridge that exists between the two tunnels. However, in this study, only three coefficients were used to analyze the phenomenon of train speed on the bridge between two tunnels in a crosswind. The coefficients were drag force, lift force, and rolling moment. Yawing moment and pitching moment were not included because their impact on the risk of overturning train was minimum.

3. Verification

3.1 Verification of Simulation Setup

The simulation was carried out by adopting the same scheme of a bridge between two tunnels in Guangzhou, China [3] which investigated the CRH3 high-speed train traveling at a speed of 250 km/h. The use of a simulation setup in the study has been compared by the results of experiments conducted by Wan and Wu [8]. The results from using the simulation setup have a difference of results below 5%. From these results it can be said that the use of the simulation setup can be justified.

Table 1 shows aerodynamics coefficient equation, where C_s, C_L, C_D, C_{RM}, C_{YM} and C_{PM} are the aerodynamic coefficients of the pressure, side force, lift force, rolling moment, yawing moment and pitching moment, respectively; $A_{SIDE}$is the area of the side face of a single carriage; A_{CROSS} is cross-sectional area of the train; V_A is the crosswind velocity relative to the running train.

From the simulation setup, this study adopted the use of boundary conditions along with the parameters used in the simulation, with the dimensions of the tunnel, bridge, and high-speed train in accordance with the conditions in Walini, West Java. This study adopted the tunnel and bridge design the same as the existing one that was built in Wallini. We also used a crosswind with a perpendicular direction with the train body to emphasize the real condition in Wallini. Simplification was also performed, the size of the simulation was scaled to 1:20.

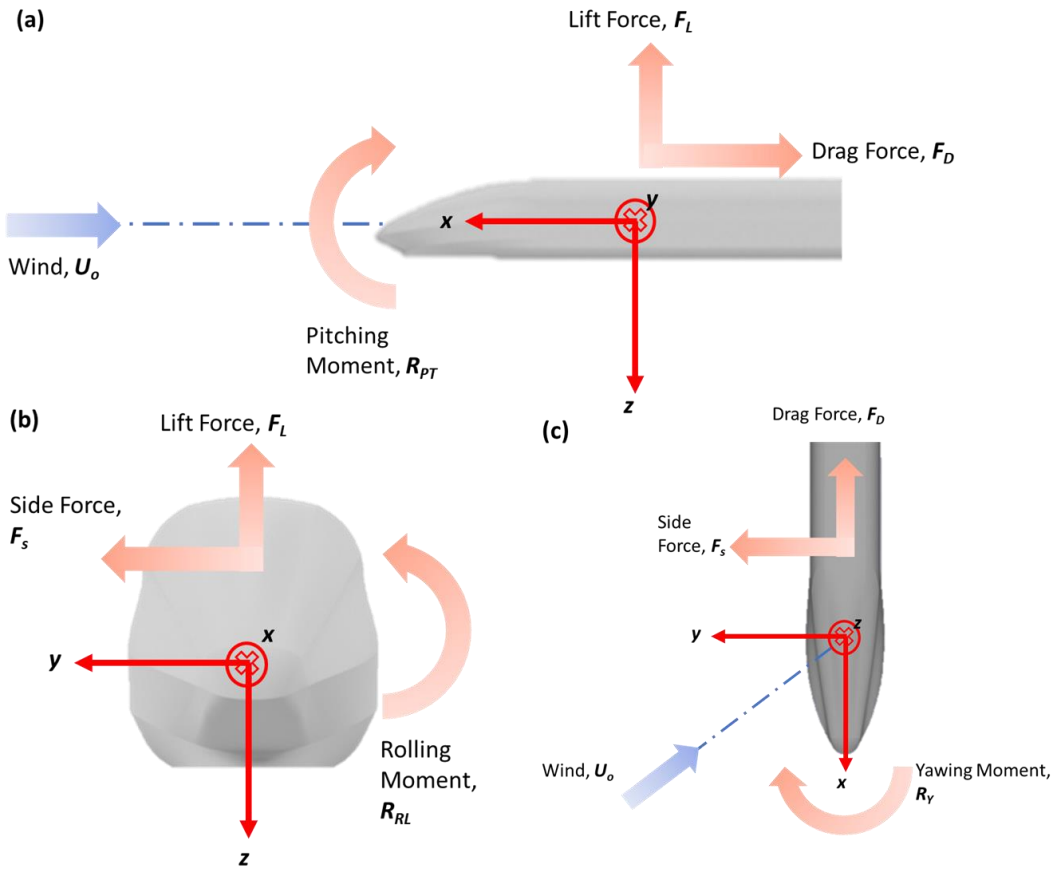

Fig. 5. Aerodynamic forces and moments act on the fast CR400AF in crosswind. (a) Side view, (b) Front view, and (c) Top view

Table 1
Aerodynamics coefficient equation

Aerodynamics coefficient	Formulation
Side force coefficient (C_s)	$C_s = \frac{F_s}{\frac{1}{2}\rho {V_A}^2 A_{SIDE}}$
Lift force coefficient (C_L)	$C_L = \frac{F_L}{\frac{1}{2}\rho {V_A}^2 A_{SIDE}}$
Drag force coefficient (C_D)	$C_D = \frac{F_D}{\frac{1}{2}\rho {V_A}^2 A_{SIDE}}$
Rolling moment coefficient (C_{RM})	$C_{RM} = \frac{R_{RM}}{\frac{1}{2}\rho {V_A}^2 A_{SIDE} h}$
Yawing moment coefficient (C_{YM})	$C_{YM} = \frac{R_{YM}}{\frac{1}{2}\rho {V_A}^2 A_{SIDE} h}$
Pitching moment coefficient (C_{PM})	$C_{PM} = \frac{R_{PM}}{\frac{1}{2}\rho {V_A}^2 A_{SIDE} h}$

3.2 Mesh Quality Check

Mesh is the main component in performing simulation calculations. The mesh used in the simulation must be accountable for the results. In ensuring these results, two methods were used to obtain the best mesh results. The first method was a mesh independent test to evaluate three mesh results with a total of 9.6, 14 and 16.5 million meshes. As shown in Table 2 the average value of lift coefficient during the simulation indicates consistent results were obtained where the grid has reached about 14 million mesh.

Table 2
Mesh independent test

Mesh quantity (million)	9.6	14	16.5
$C_{L\ Average}$	0.051	0.029	0.031

The second method was to reduce the skewness result. Skewness itself affects the shape of the mesh and will directly affect the calculations to be performed in the simulation. High Skewness will make the simulation results inaccurate. The skewness criteria as shown Table 3, where the smaller the skewness value, the better the mesh results. Various meshing methods can be used to reduce the skewness results obtained. In this study, the results of the mesh obtained are 14 million with an average skewness of 0.22. From the skewed results, the mesh results are consistent.

Table 3
Skewness quality

Value of Skewness	Cell quality
0.9 - 1	*Bad*
0.75 - 0.9	*Poor*
0.5 - 0.75	*Fair*
0.25 - 0.5	*Good*
0 - 0.25	*Excellent*

4. Result and Discussion

4.1 Aerodynamics Coefficient

The aerodynamic coefficients obtained are plotted in the graph contains 550 data points of aerodynamic coefficients along the route taken by the CR400AF train. The 550 plot points represent every aerodynamic coefficient on the CR400AF fast train. Each time step represents a movement of 0.0973 m in the simulation or 1.94 m in real scale. Hence, each observation will be based on a 1.94 m displacement of the train on a real scale.

4.1.1 Drag coefficient

In Figure 6(a) it can be seen how the behavior of the drag coefficients on the simulation route. The graph is divided into four regions, which focus on the bridge region (BR). On the drag coefficient, it can be seen several important observations. The drag in the area without crosswind is stable at 0.18 – 0.20. The drag in the tunnel is due to the piston effect which makes the pressure increase in the area of the train body. The rise of coefficient drag about to 0.3 in tunnel 7 (T1) and 0.42 – 0.6 in tunnel 8 walini (T2) (depending on the crosswind). In the bridge region coefficient drag increases in

line with the increase in crosswind. The increase of the drag is 1.39 times with the crosswind velocity of 10 m/s, and 1.67 times with the crosswind velocity of 25 m/s. Furthermore, the drag coefficient will stabilize at 0.18 – 0.20 after entering the tunnel and is not affected by crosswind.

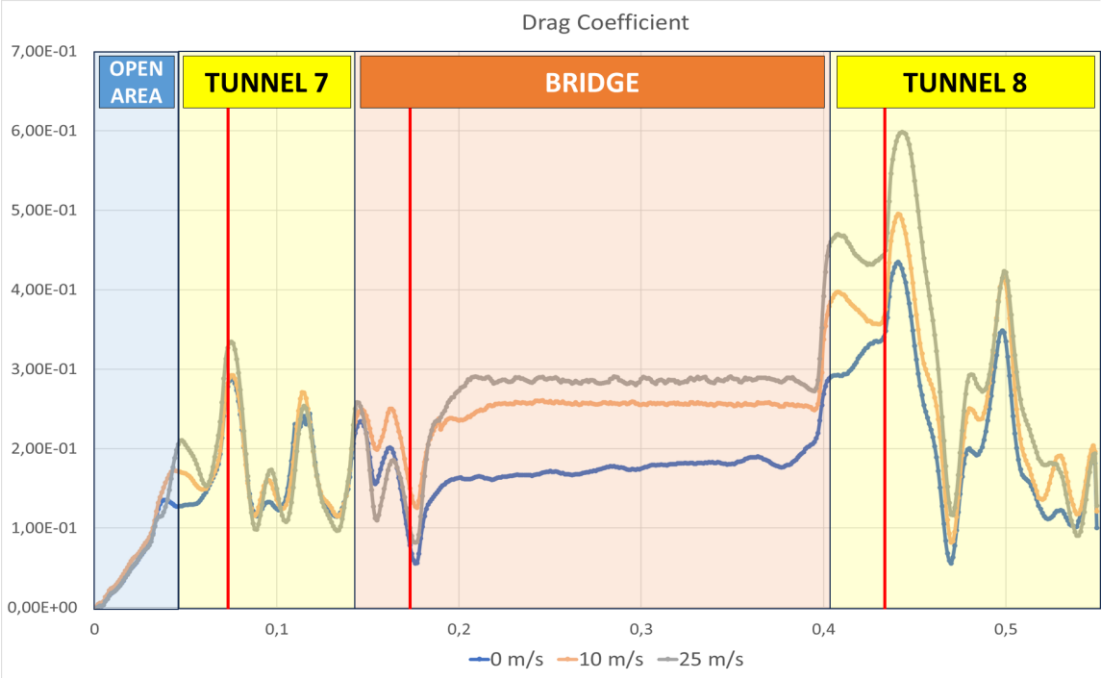

(a)

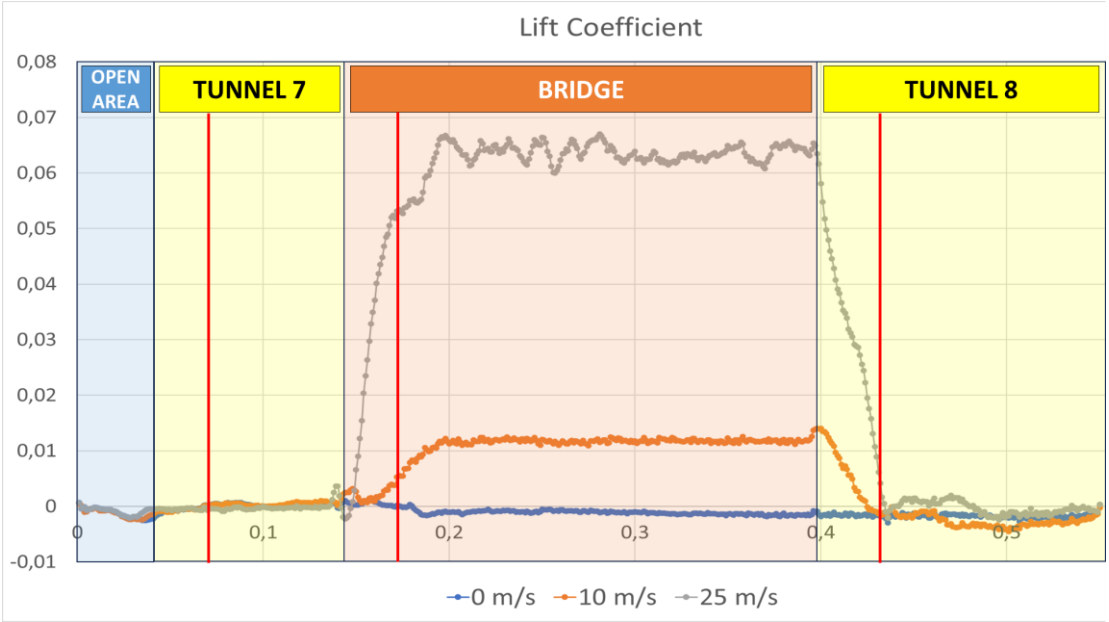

(b)

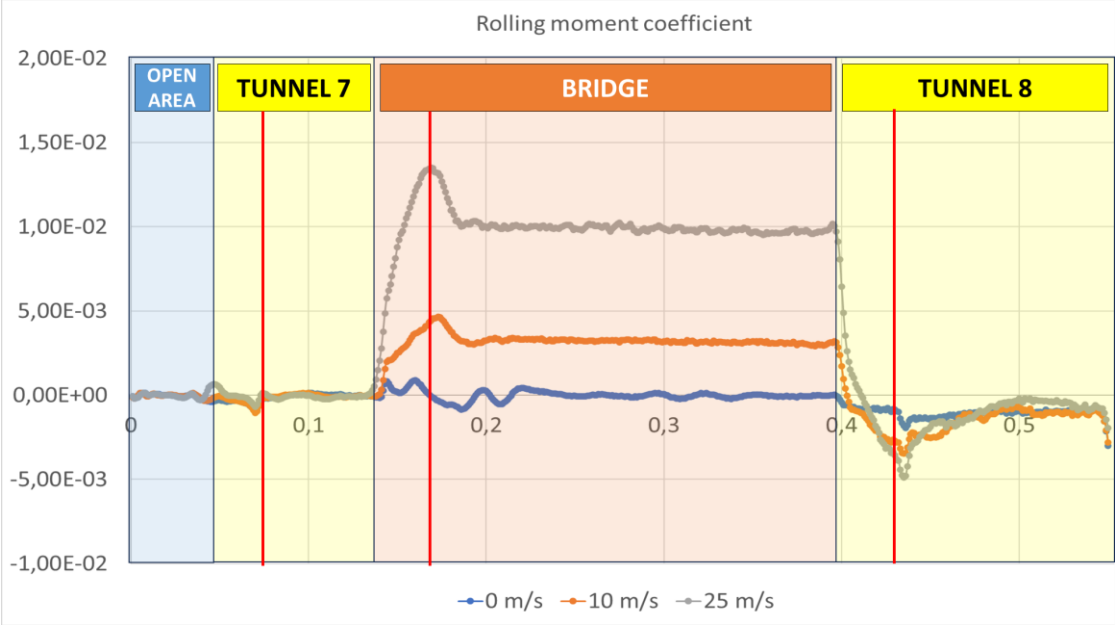

(c)

Fig. 6. Drag coefficient (a) Lift coefficient (b) Rolling moment coefficient (c) Values with variation of crosswind and coefficient values on top of bridge

4.1.2 Lift coefficient

Figure 6(b) shows the coefficient lift along the simulation route. It can be seen that the lift is not too affected by the shape of the tunnel so it does not change too much, this is due to lift which only affects fluid velocity and design of the train geometry. In the "IN" and "OUT" processes the lift fluctuates when there is a crosswind, this fluctuation occurs during the process of the train body entering the bridge region. When the train is completely on the bridge, the lift will tend to be stable although it will be larger with the crosswind. This is due to the fluid hitting the train from the side. The increase in the coefficient is very large, reaching 10.6 times in the crosswind 10 m/s and 59.8 times in the crosswind 25 m/s.

4.1.3 Rolling moment coefficient

In Figure 6(c), it can be figured out that the rolling moment, just like the lift coefficient, does not have much effect when entering the tunnel. While, when on the bridge, especially in the "IN" and in the “OUT” process, the aerodynamic load on the train will increase by 5.88 times at a crosswind 10 m/s and 18.8 times at a crosswind 25 m/s. The external force caused by crosswind changes the rolling moment.

4.2 “IN” and “OUT” Process Comparison

The “IN” process and the “OUT” process will also be discussed by comparing the fluctuations that occur in the process. We use a simple formula as follows:

$$\Delta C = C_{max} - C_{min} \tag{3}$$

It can be seen in Table 4 that the "OUT" process has a higher fluctuation than the "IN" process because the results of the comparison of IN/OUT is less than one (< 1). However, the two processes will not have a significant difference if there is no crosswind at all. So, it can be concloude that crosswind give high impact to both “IN” and “OUT” process.

Table 4
Comparison of maximum fluctuation amplitudes of aerodynamic coefficients under different conditions of crosswind velocities

Aerodynamics coefficients	Crosswind velocity	Cmax - Cmin		IN/OUT
		IN	OUT	
Drag coefficient	*0 m/s*	0.1787	0.1729	1.03
	10 m/s	0.1641	0.2459	0.67
	25 m/s	0.1763	0.3147	0.56
Lift force coefficient	*0 m/s*	0.0023	0.0021	1.09
	10 m/s	0.0113	0.0161	0.71
	25 m/s	0.0607	0.0710	0.85
Rolling moment coefficient	*0 m/s*	0.0016	0.0016	1.00
	10 m/s	0.0047	0.0067	0.71
	25 m/s	0.0111	0.0126	0.88

4.3 Pressure Contour Top View

In the following discussion, the pressure contour analysis is carried out for three conditions i.e. the "IN", "MID", and "OUT" processes to compare the conditions when there is a crosswind and no crosswind. The “IN” process is represented by analysis when the train body is between 2 regions, namely tunnel 7 (T1) and bridge region (BR). Analysis of the "IN" process was carried out using 4 locations, each 1 meter apart. The “MID” process is representative of all the train bodies at the bridge and uses 3 location points 1.5 m apart to represent the head, middle and tail. The “OUT” process is analyzed when the train position is between the bridge region and tunnel walini.

Under crosswind conditions as shown in Figure 7 a(1)-(2) there is a pressure difference between tunnel region 7 (T1) and bridge region (BR), the negative pressure generated in the tunnel region is greater than the condition that there is no crosswind as shown in Figure 7 b(1)-(2). This is because the tunnel that has a lower pressure creates a suction chamber for crosswind flow into the tunnel. That way, the compression wave that occurs will be larger.

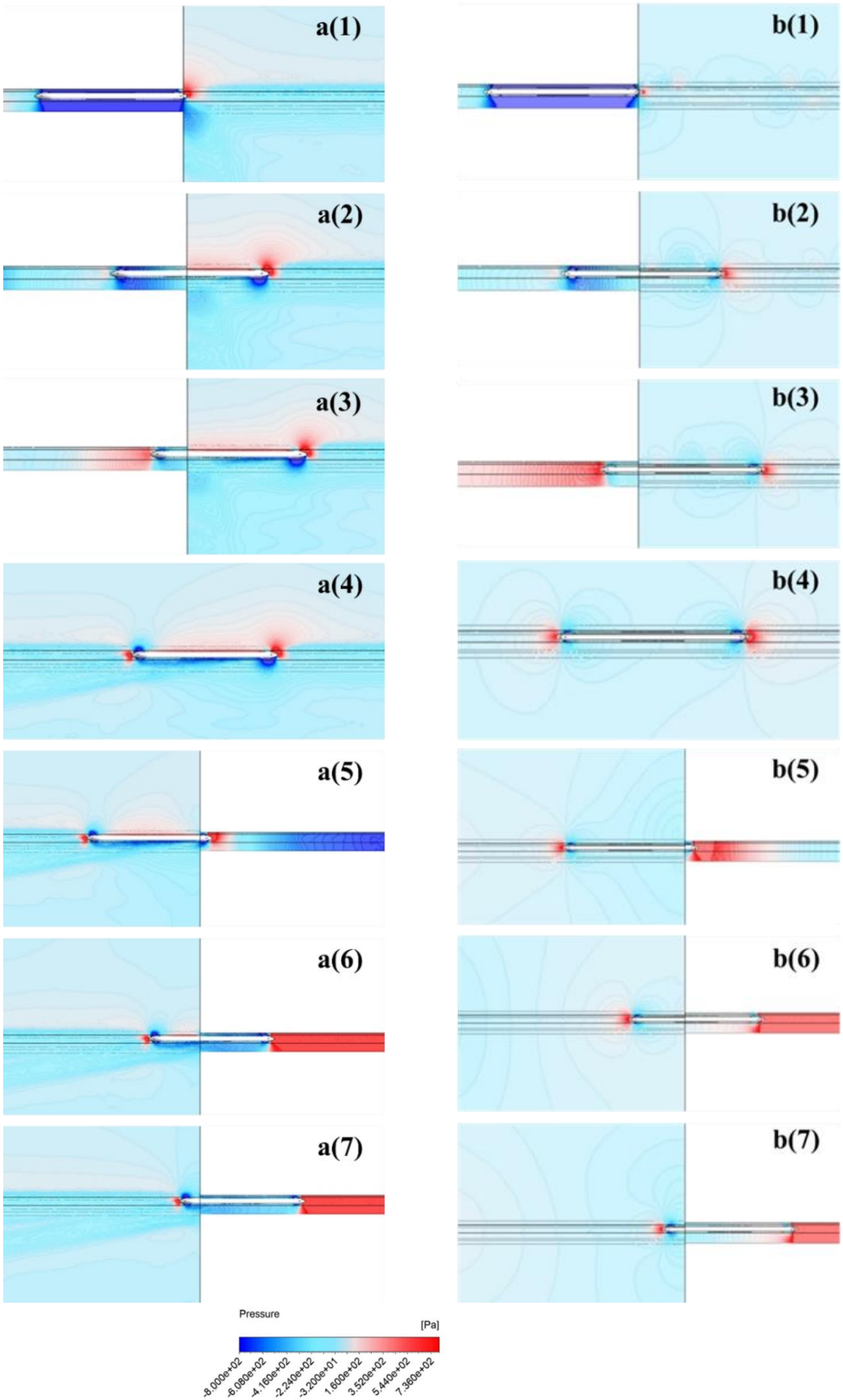

Fig. 7. Pressure contour with crosswind (a) Without crosswind (b) "IN" a(1)-(3) & b(1)-(3) "MID" a(4) & b(4) "OUT" a(5)-(7) & b(5)-(7)

The pressure increase in the head is very different when compared between the two conditions. Under crosswind conditions as shown in Figure 7a (1)-(3), the head of the train experiences a greater pressure increase on the windward side and a pressure drop on the leeward side of the train. This is obviously caused by a crosswind hitting the body of the train. In the "MID" process, all parts of the train have been in the bridge region (BR). In Figure 7a (4), the difference in pressure on both sides of the train makes the flow on the train asymmetrical. In contrast to trains without crosswinds shown in Figure 7b (4), it can be observed that there are symmetrical flows on both sides of the train.

The "OUT" process begins when the train begins to enter the territory of tunnel 8 walini (T2). In Figure 7a (5)-(7) it is seen that there is a greater pressure difference compared to no crosswind in Figure 7b (5)-(7). Negative pressure in the leeward area of the train is formed as shown in the figure which will allow the occurrence of a longitudinal conical vortex which is formed from the results of circumferential flow due to crosswind and circumferential flow generated from a running train [3]. The longitudinal conical vortex formed in the crosswind state will be cut off when it enters tunnel 8 walini. Fluctuations in the results of aerodynamic coefficients when entering tunnel 8 walini (T2) are caused by the presence of jet flow resulting from the direction of movement of the train. In the crosswind condition, it will produce a jet flow that is greater than no crosswind. The resulting jet flow will follow into tunnel 8 walini (T2) which may be the main reason for fluctuations in aerodynamic coefficients.

4.4 Pressure Contour Cross-sectional View

From Figure 8, it is obvious that during "IN" process, the difference in pressure field is very noticeable when the train part is already on the bridge. This is very clearly seen when the crosswind condition is formed high pressure on the windward side of the train and produces negative pressure on the leeward side of the train, while when there is no crosswind, it will not be too noticeable the formation of negative pressure when it is over the bridge. There is also a pressure difference that occurs when the train is in the tunnel. However, this difference is not very significant. In this case, the negative pressure in the crosswind condition is greater. In the "MID" process, it can be seen the distribution of aerodynamic loads on the train. Where on Figure 9 it appears that the head section on the train has a greater pressure distribution than the middle and tail in both conditions. Moreover, in the "OUT" process shown in Figure 10, there is a much greater pressure difference than the "IN" process. This is because of the possibility of the occurrence of a longitudinal conical vortex during a crosswind state so that when it is about to enter tunnel 8 walini (T2) it makes the longitudinal conical vortex restrained. This is what will make the "OUT" process have greater fluctuations in aerodynamic loads. The difference is also seen in the tunnel region where there is a non-negative pressure region in the state of no crosswind. The opposite is indicated in the crosswind state where the negative pressure region obtained is greater.

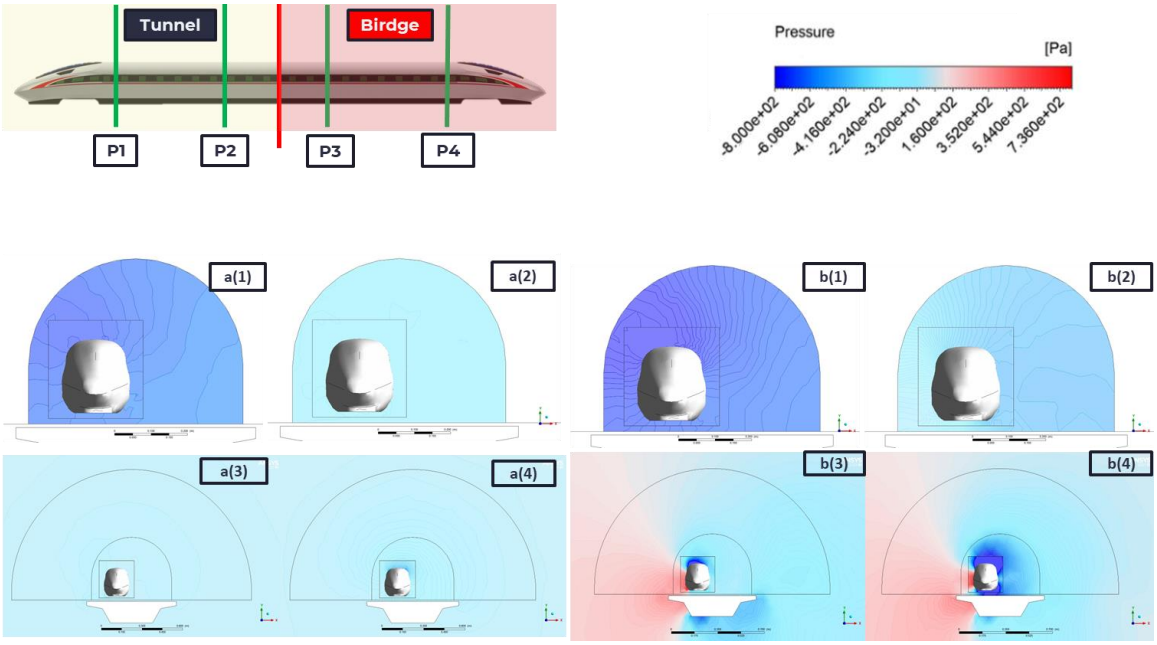

Fig. 8. Pressure contour "IN" process under no crosswind a(1)-(4) and crosswind 25 m/s b(1)-(4)

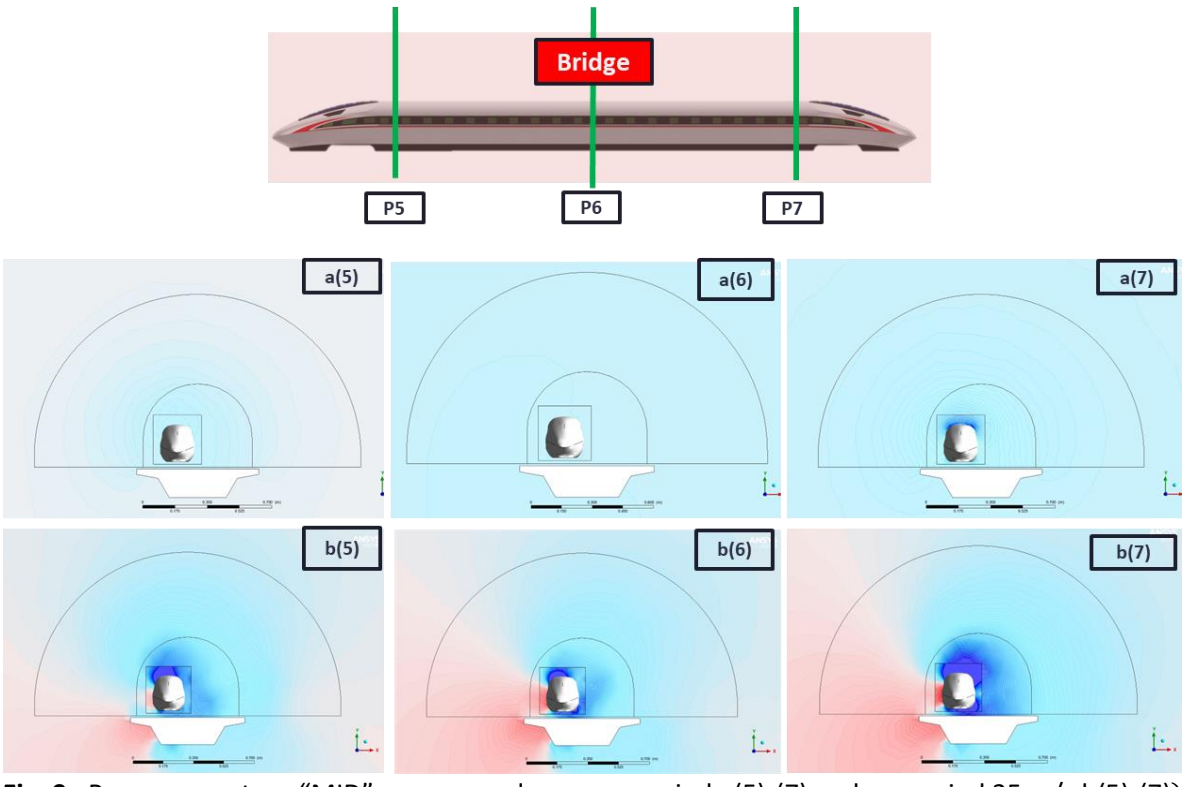

Fig. 9. Pressure contour “MID” process under no crosswind a(5)-(7) and crosswind 25 m/s b(5)-(7))

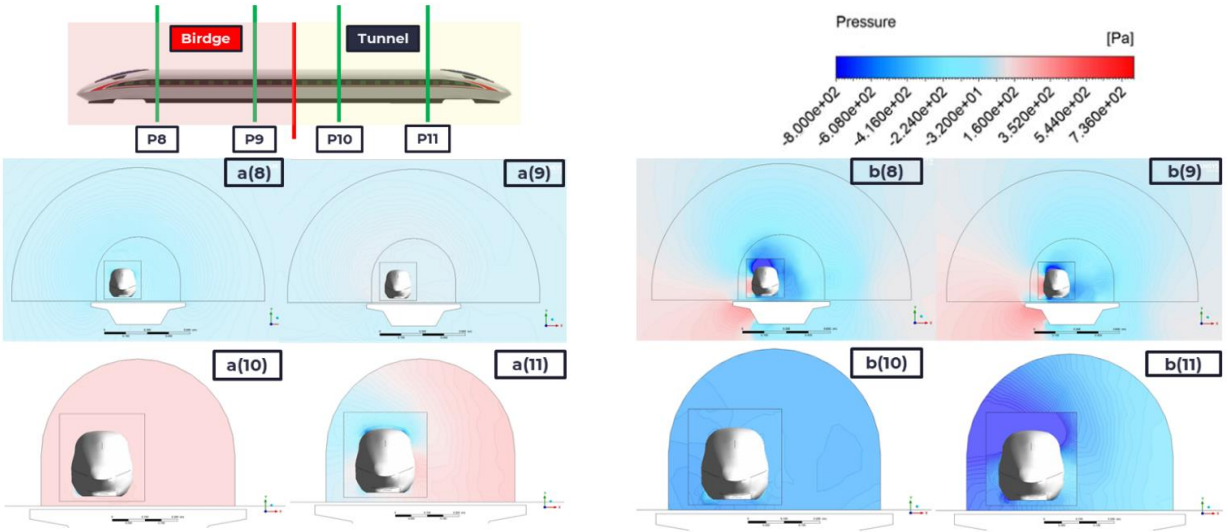

Fig. 10. Pressure contour "OUT" process under no crosswind $(a_{(8-11)})$ and crosswind 25 m/s $(b_{(8-11)})$

5. Conclusions

Based on simulations and analyzes that have been carried out on the influence of crosswinds on trains passing on tunnel routes – bridges – tunnels on aerodynamic performance on trains, it can be concluded several important points as follows:

i. The difference that exists when there is a crosswind is very noticeable in the pressure caused by the crosswind on the windward and negative pressure in the leeward area. Pressure is the main reason for the change in the aerodynamic coefficient because the train acts as a bluff body.

ii. In the crosswind state, the three aerodynamic coefficients have the following behavior:
   a. The drag coefficient is not greatly affected by the presence of crosswinds in the "IN" and "OUT" processes. This can be seen because the fluctuations that occur in the "IN" process have the same behavior in the existing crosswind variations. Meanwhile, in the "OUT" process, there is an increase in the peak point of the drag coefficient as the crosswind speed increases. This means that the crosswind will affect the drag coefficient when the train is on the bridge and the "OUT" process because it increases 1.39 times on the 10 m/s crosswind and 1.67 times on the 25 m/s crosswind.
   b. The coefficient of lift greatly affects the "IN" process and the "OUT" process. This is indicated by the difference of 10.6 times greater in the 10 m/s crosswind and 59.8 times on the 25 m/s crosswind.
   c. The rolling moment coefficient greatly affects the "IN" process and the "OUT" process. This is indicated by an increase of 18.8 times on a 10 m/s crosswind and 25.7 times on a 25 m/s crosswind.

iii. The "OUT" process has greater fluctuations in aerodynamic loads compared to the "IN" process. This is because there is a jetflow that allows the longitudinal conical vortex to occur and will break when entering tunnel 8 walini (T2)

iv. The head section on the train experiences the greatest aerodynamic load, indicated by the pressure difference between the two sides of the train. Followed by the tail section of the train and finally the middle part of the train which has a role in the load of the smallest aerodynamic coefficient.

Acknowledgments

This research was supported by Faculty of Engineering Universitas Indonesia under Seed Funding for Professor Research Fiscal Year 2022/2023, No.NKB-1942/UN2.F4.D/PPM.00.00/2022

References

[1] de Rus Mendoza, Ginés. *Economic analysis of high speed rail in Europe*. Fundacion BBVA, 2012.

[2] Baker, C. J. "A review of train aerodynamics Part 1–Fundamentals." *The Aeronautical Journal* 118, no. 1201 (2014): 201-228. https://doi.org/10.1017/S000192400000909X

[3] Deng, E., Weichao Yang, Lu Deng, Zhihui Zhu, Xuhui He, and Ang Wang. "Time-resolved aerodynamic loads on high-speed trains during running on a tunnel–bridge–tunnel infrastructure under crosswind." *Engineering Applications of Computational Fluid Mechanics* 14, no. 1 (2020): 202-221. https://doi.org/10.1080/19942060.2019.1705396

[4] Li, Yongle, Peng Hu, Xinyu Xu, and Junjie Qiu. "Wind characteristics at bridge site in a deep-cutting gorge by wind tunnel test." *Journal of Wind Engineering and Industrial Aerodynamics* 160 (2017): 30-46. https://doi.org/10.1016/j.jweia.2016.11.002

[5] Deng, E., Weichao Yang, Mingfeng Lei, Zhihui Zhu, and Pingping Zhang. "Aerodynamic loads and traffic safety of high-speed trains when passing through two windproof facilities under crosswind: A comparative study." *Engineering Structures* 188 (2019): 320-339. https://doi.org/10.1016/j.engstruct.2019.01.080

[6] Baker, C. J. "The simulation of unsteady aerodynamic cross wind forces on trains." *Journal of wind engineering and industrial aerodynamics* 98, no. 2 (2010): 88-99. https://doi.org/10.1016/j.jweia.2009.09.006

[7] Cheng, S. Y., Makoto Tsubokura, Takuji Nakashima, Takahide Nouzawa, and Yoshihiro Okada. "A numerical analysis of transient flow past road vehicles subjected to pitching oscillation." *Journal of Wind Engineering and Industrial Aerodynamics* 99, no. 5 (2011): 511-522. https://doi.org/10.1016/j.jweia.2011.02.001

[8] Wan, X. Y., and Jian Wu. "In-situ test and study on the aerodynamic effect of the rolling stock passing through tunnels with a speed of 200 km/h." *Modern Tunnelling Technology* 143, no. 1 (2006): 43-48.

[9] Han, K., and H. Q. Tian. "Research and application of testing technology of aerodynamics at train-tunnel entry on special passenger railway lines." *J. Cent. South Univ. Sci. Technol* 38 (2007): 326-332.

[10] Yang, Weichao, E. Deng, Mingfeng Lei, Pingping Zhang, and Rongshen Yin. "Flow structure and aerodynamic behavior evolution during train entering tunnel with entrance in crosswind." *Journal of Wind Engineering and Industrial Aerodynamics* 175 (2018): 229-243. https://doi.org/10.1016/j.jweia.2018.01.018

[11] Chen, Feng, Haorong Peng, Xiaoxiang Ma, Jieyu Liang, Wei Hao, and Xiaodong Pan. "Examining the safety of trucks under crosswind at bridge-tunnel section: A driving simulator study." *Tunnelling and Underground Space Technology* 92 (2019): 103034. https://doi.org/10.1016/j.tust.2019.103034

[12] Niu, Ji-qiang, Dan Zhou, Xi-feng Liang, Scarlett Liu, and Tang-hong Liu. "Numerical simulation of the Reynolds number effect on the aerodynamic pressure in tunnels." *Journal of Wind Engineering and Industrial Aerodynamics* 173 (2018): 187-198. https://doi.org/10.1016/j.jweia.2017.12.013

[13] Suzuki, Masahiro. "Flow-induced vibration of high-speed trains in tunnels." In *The Aerodynamics of Heavy Vehicles: Trucks, Buses, and Trains*, pp. 443-452. Springer Berlin Heidelberg, 2004. https://doi.org/10.1007/978-3-540-44419-0_39

[14] Niu, Jiqiang, Dan Zhou, Xifeng Liang, Tanghong Liu, and Scarlett Liu. "Numerical study on the aerodynamic pressure of a metro train running between two adjacent platforms." *Tunnelling and Underground Space Technology* 65 (2017): 187-199. https://doi.org/10.1016/j.tust.2017.03.006

[15] Yang, Weichao, E. Deng, Mingfeng Lei, Zhihui Zhu, and Pingping Zhang. "Transient aerodynamic performance of high-speed trains when passing through two windproof facilities under crosswinds: A comparative study." *Engineering Structures* 188 (2019): 729-744. https://doi.org/10.1016/j.engstruct.2019.03.070

[16] Chen, Zheng-Wei, Tang-Hong Liu, Chun-Guang Yan, Miao Yu, Zi-Jian Guo, and Tian-Tian Wang. "Numerical simulation and comparison of the slipstreams of trains with different nose lengths under crosswind." *Journal of Wind Engineering and Industrial Aerodynamics* 190 (2019): 256-272. https://doi.org/10.1016/j.jweia.2019.05.005

[17] Lu, Yibin, Tiantian Wang, Mingzhi Yang, and Bosen Qian. "The influence of reduced cross-section on pressure transients from high-speed trains intersecting in a tunnel." *Journal of Wind Engineering and Industrial Aerodynamics* 201 (2020): 104161. https://doi.org/10.1016/j.jweia.2020.104161

[18] AbdelGawad, Ahmed Farouk, Naser Mohammed Aljameel, and Ramy Elsayed Shaltout. "Computational Modelling of the Aerodynamic Noise of the Full-Scale Pantograph of High-Speed Trains." *Journal of Advanced Research in Fluid Mechanics and Thermal Sciences* 93, no. 1 (2022): 94-109. https://doi.org/10.37934/arfmts.93.1.94109

[19] Wang, Shibo, James R. Bell, David Burton, Astrid H. Herbst, John Sheridan, and Mark C. Thompson. "The performance of different turbulence models (URANS, SAS and DES) for predicting high-speed train slipstream." *Journal of Wind Engineering and Industrial Aerodynamics* 165 (2017): 46-57. https://doi.org/10.1016/j.jweia.2017.03.001

[20] Ishak, Izuan Amin, Mohamed Sukri Mat Ali, Mohamad Fitri Mohd Yakub, and Sheikh Ahmad Zaki Shaikh Salim. "Effect of crosswinds on aerodynamic characteristics around a generic train model." *International Journal of Rail Transportation* 7, no. 1 (2019): 23-54. https://doi.org/10.1080/23248378.2018.1424573